Applied Physics Letters

Room-temperature photoluminescence and electroluminescence of 1.3-μm-range BGaInAs quantum wells on GaAs substrates

Cite as: Appl. Phys. Lett. **117**, 021102 (2020); https://doi.org/10.1063/5.0011147
Submitted: 17 April 2020 . Accepted: 27 June 2020 . Published Online: 13 July 2020

R. H. El-Jaroudi, K. M. McNicholas, A. F. Briggs, S. D. Sifferman, L. Nordin, and S. R. Bank

Applied Physics Letters ARTICLE scitation.org/journal/apl

Room-temperature photoluminescence and electroluminescence of 1.3-μm-range BGaInAs quantum wells on GaAs substrates

Cite as: Appl. Phys. Lett. **117**, 021102 (2020); doi: 10.1063/5.0011147
Submitted: 17 April 2020 · Accepted: 27 June 2020 ·
Published Online: 13 July 2020

R. H. El-Jaroudi,[a] K. M. McNicholas, A. F. Briggs, S. D. Sifferman, L. Nordin, and S. R. Bank[a]

AFFILIATIONS

Microelectronics Research Center, Electrical and Computer Engineering, The University of Texas at Austin, 10100 Burnet Rd., Austin, Texas 78752, USA

[a]**Authors to whom correspondence should be addressed:** reljaroudi@utexas.edu and sbank@ece.utexas.edu

ABSTRACT

We report the room temperature photoluminescence and electroluminescence properties of boron incorporated into highly strained InGaAs, forming BGaInAs, grown on GaAs substrates. X-ray diffraction was used to determine the alloy composition and strain of BGaInAs quantum wells on GaAs. As expected, the addition of boron reduced the quantum well compressive strain, preventing strain-relaxation and enabling extension of the peak emission wavelength of InGaAs quantum wells to 1.3 μm on GaAs. We also report both the longest wavelength emission observed from BGaInAs (1.4 μm) and electrically injected photoemission from a dilute-boride active region. We observed a blueshift in electroluminescence, due to unintentional *in situ* annealing of the active region, which we mitigated to demonstrate a path to realize true 1.3 μm emitters in the presence of *in situ* annealing.

Near-infrared (NIR, 1–3 μm) emitters are important for a wide range of high-volume applications such as telecommunications, LiDAR, and facial recognition. GaAs-based vertical cavity surface-emitting lasers (VCSELs) offer an inexpensive solution at these wavelengths as they leverage the monolithic integration of AlGaAs-GaAs distributed Bragg reflectors and AlO_x native oxide technologies. However, few active regions are available nearly lattice matched to GaAs at these wavelengths. NIR emitters have been demonstrated at 1.3 μm utilizing In(Ga)As quantum dots[1] (QDs) or InGaNAs[2] active regions. The comparatively low modulation bandwidth of InAs QD lasers emitting at 1.3 μm (Ref. 3) and the difficulty in promoting the substitutional incorporation of nitrogen in InGaAs quantum wells (QW)[4] motivate the search for an alternative active region. Similar to dilute nitrides, in which the small lattice constant and favorable band anti-crossing are exploited to reduce the strain and extend the emission wavelength of InGaAs on GaAs,[5] the addition of boron can be used to reduce the strain of highly compressively strained InGaAs QWs required to reach NIR wavelengths on GaAs. The advantage of dilute borides over the dilute nitrides is a predicted higher solid solubility of boron than nitrogen, enabling higher incorporation and simplified growth of dilute-boride alloys compared to nitride alloys.[6]

While the growth of dilute borides on GaAs has been previously demonstrated by several groups,[7–16] the growth of boron pnictides has proven to be more challenging than other III–V material systems. These challenges are due to the high melting point and low vapor pressure of boron, the stable sub-pnictide phase of B-V materials, and the large lattice mismatch between B-V binaries and conventional substrates.[17] Recent progress in the epitaxial growth of B-III-V alloys has focused on increasing the substitutional incorporation of boron.[7] While the theoretical estimates predict that boron has a higher solid solubility in GaAs than nitrogen,[6] most demonstrations of B-III-V remain limited to low concentrations of B. Previous alloy concentrations have been restricted to high In concentrations (∼40%) and low boron concentrations (∼2%) or low In (∼6%) and higher B (∼5%) concentrations.[8–10] The difficulty in simultaneously incorporating high indium and high boron concentrations has limited the emission wavelength of BGaInAs alloys to <1.2 μm.[8–13] As with other highly mismatched alloys, the key to improving material quality is optimizing the growth regime to promote the substitutional incorporation of B. Combining the effects of low substrate temperature ($\leq 400\,^{\circ}C$)[7] and Bi as a surfactant,[14] we have recently demonstrated a highly kinetically limited growth regime allowing us to incorporate higher B (>12%) concentrations in BGaAs.[18] Here, we tailored the same approach to

increase the solid solubility of B in InGaAs, extending the photoluminescence (PL) emission wavelength from a dilute-boride QW beyond 1.2 μm and demonstrating electroluminescence (EL) from a boron-containing active region electrically injected emitter.

Samples were grown in an EPI Mod Gen II solid-source molecular beam epitaxy (MBE) system equipped with a Veeco Mark IV valved cracker for arsenic, Veeco SUMO effusion cells for gallium and indium, and an MBE Komponenten electron-beam evaporation boron source. The B e-beam source was operated at powers between 70 and 120 W depending on the desired B flux, with a figure-8 raster pattern. *In situ* characterization of the surface was limited during QW growth due to interference between the boron electron beam and the reflection high-energy electron diffraction (RHEED) electron beam. However, the "streaky" RHEED patterns indicative of 2D growth were observed after the e-beam was turned off. The substrate temperature was 380 °C as measured by pyrometry. Photoluminescence structures with a 200 nm GaAs buffer, a 10 nm (B)GaInAs QW, and a 50 nm GaAs cap were grown on an on-axis semi-insulating (100) GaAs substrate. The As_2:Ga flux ratio was ~3 (beam equivalent pressure ratio of 15). The GaAs growth rate was 1.3 Å/s, and the BGaInAs growth rate was ~2.5–3 Å/s. BGaInAs compositions were determined using a combination of calibrations of the constituent ternaries, InGaAs and BGaAs, as well as post-growth metrology. Specifically, InGaAs/GaAs superlattices were grown to determine the relationship between relative Ga/In fluxes, cell temperatures, and the resulting alloy compositions. BGaAs films were grown to determine the relationship between the boron flux and e-beam power, assuming Vegard's law as per Ptak *et al.*[14] Secondary ion mass spectrometry (SIMS) confirmed the unity sticking growth regime of both the BGaAs and BGaInAs alloys, enabling alloy compositions to be determined by high-resolution x-ray diffraction (HR-XRD) ω-2θ coupled-scan analysis about the (004) reflection of GaAs using a Rigaku SmartLab HR-XRD.[19,20] Based upon the ternary alloy beam-equivalent pressure (BEP) to flux calibrations, prior to growth, *in situ* BEP measurements were used to determine the In and Ga fluxes and achieve the desired In:Ga flux ratio. Due to incompatibility between the beam flux ion gauge and elemental boron, HR-XRD was performed during post-growth to confirm the B concentrations as well as the QW strain. Photoluminescence was measured using a Nd:YAG laser at 532 nm, a 0.5 mm grating spectrometer, and a thermoelectric-cooled InGaAs detector. Reported spectra were all measured compared to a standard sample to facilitate a direct comparison of PL intensity and wavelength across samples.

Our approach was similar to that of Tansu *et al.*,[21] we increased the In concentration in InGaAs QWs on GaAs until no PL was observed (~40% In). We then grew BGaInAs QWs at that In concentration in order to reduce the compressive strain in the QWs. Figure 1 shows the effects of increasing indium and boron concentration on the structural and optical quality of (B)GaInAs quantum wells. As shown in the room temperature PL of the InGaAs QWs [Fig. 1(b)], increasing the indium concentration resulted in a severe degradation of the material optical quality, such that no PL was observed. This increase in the indium concentration also resulted in a reduction in crystalline quality as observed in HR-XRD [Fig. 1(c)] through the complete loss of the previously well-defined finite thickness fringes, as well as broadening of the QW peak in the higher In concentration QW. The addition of 2%–6% boron reduced the compressive strain (from approximately −3% without B to between approximately −2.7% and −2.1%) in the material, as indicated by the shift of the QW peak to larger diffraction angles with increasing B in HR-XRD. The recovery of well-defined thickness fringes and QW peaks suggest improved structural quality. In PL, optical quality material was recovered and the desired wavelength extension to 1.3 μm was observed [Fig. 1(b)]. Additionally, the decrease in optical quality with the addition of 2% B was not as severe as that observed in the dilute nitrides, where the addition of even 1% nitrogen significantly degraded the optical quality of the material.[22,23]

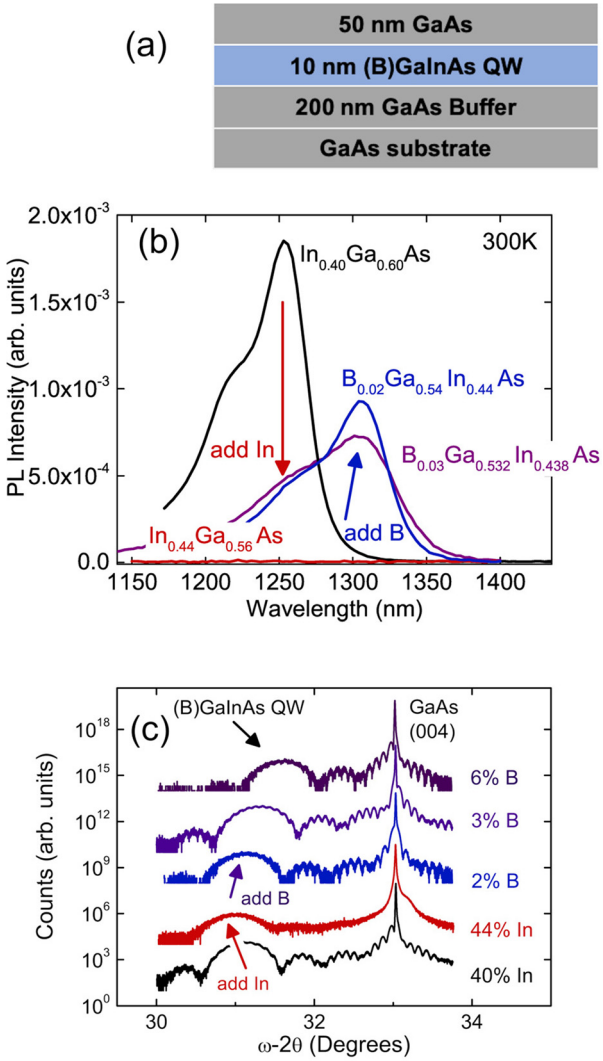

FIG. 1. (a) Layer structure of the (B)GaInAs PL samples. (b) PL of the (B)GaInAs QWs on GaAs targeting 1.3 μm emission. Increasing the In concentration of the InGaAs QW resulted in a complete loss of PL strength. With the addition of 2% B, a strong emission peak at 1.3 μm was observed. (c) HR-XRD of (B)GaInAs QWs on GaAs. A loss of well-defined finite thickness fringes and well-defined QW peak was observed as the In concentration was increased. With the addition of B, a recovery of thickness fringes and well-defined QW peak suggests improved structural quality from the reduction in strain.

To demonstrate the potential for B-containing optoelectronic devices, we grew a nominally identical $B_{0.02}Ga_{0.54}In_{0.44}As$ active region

between n- and p-type AlGaAs contact layers. The EL structure was grown on n-type (100) GaAs substrates. The n-contact (Si-doped) layer of the EL structures was grown in a Varian Gen II solid-source MBE system equipped with an aluminum cell, As-capped, and transferred *in situ* to the MBE with the boron cell for the growth of the active region under the same growth conditions as described previously. The sample was then As-capped and transferred *in situ* back to the Al-containing MBE for the growth of the p-contact (Be-doped) layer. The AlGaAs growth temperature was 580 °C, as measured by kSA BandIt blackbody thermometry, and the growth rate was 3 Å/s.

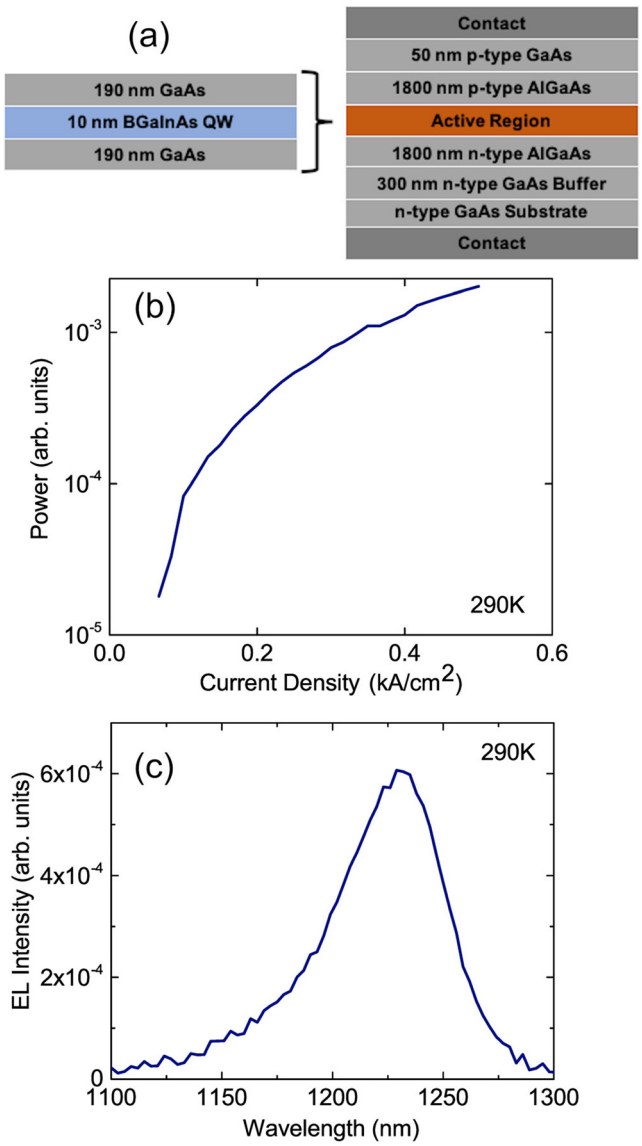

FIG. 2. (a) Layer structure of the EL structure with a BGaInAs QW active region. (b) Light output vs input current (L-I) curve and (c) emission spectra (at $J = 0.5$ kA/cm^2) of the boron-containing active region electrically injected emitter. While the nominally identical PL structure with ∼2% B and ∼44% In emitted at 1.3 μm, a blueshift in the wavelength to <1.25 μm was observed in the EL structure.

Electroluminescence was measured at room temperature using an InGaAs detector, under pulsed conditions with a 1% duty cycle. The sample structure, light-output vs input current (L–I) curve, and emission spectrum are shown in Fig. 2. While the thin PL structure emitted at 1.3 μm, the otherwise identical active region embedded in the EL structure emitted at <1.25 μm. A similar blueshift is observed in dilute-nitride device growth due to thermal annealing of the active region.[24–26] *In situ* annealing of a BGaInAs PL structure of near identical composition, but grown under different growth conditions, also exhibited a blueshift in the wavelength and an increase in PL intensity. Therefore, we performed *ex situ* annealing on the PL structure [Fig. 1(a)] to understand the effects on the active region of the high growth temperature required to grow the AlGaAs p-type contact layer. Rapid thermal annealing (RTA) allows for *ex situ* annealing of samples in order to examine the effects of annealing. Annealing conditions were chosen to observe the increase in PL intensity and blueshift in the wavelength observed in the EL structure. While *ex situ* annealing does not allow for a direct comparison of temperature and time to *in situ* annealing, it facilitates further understanding of thermal annealing effects without the restrictions (time, sample size, and cleanliness) of *in situ* annealing. The sample was placed on a Si carrier wafer, and a GaAs proximity cap wafer was placed on top in order to prevent As out-diffusion from the sample. The temperature was monitored using a pyrometer below the Si carrier wafer. The identical PL structure was annealed at temperatures from 550 °C to 750 °C for one minute. As shown in Fig. 3, annealing of the QW resulted in a blueshift of the emission wavelength comparable to that of the EL structure. In the dilute nitrides, this blueshift in the wavelength has been attributed to the rearrangement of In-N nearest neighbors.[25,26] Further investigation is required to better understand the root cause(s) in the dilute borides.

Annealing of the QW also resulted in over an order of magnitude improvement in PL intensity (Fig 3). Similar to the dilute nitrides,[24–28] thermal annealing appears to be crucial for high luminescence efficiency in the dilute borides. However, the accompanying blueshift in the emission wavelength necessitates increasing the as-grown emission

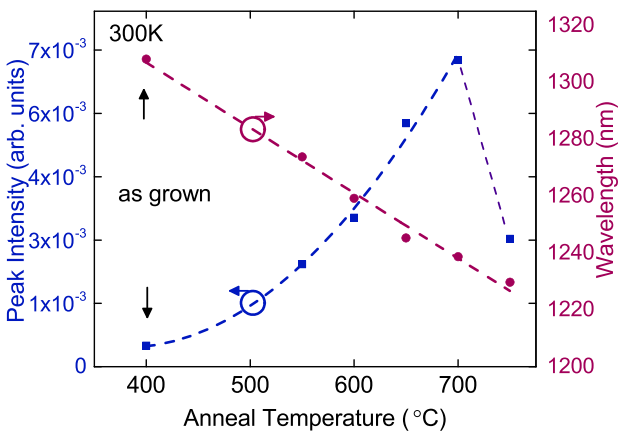

FIG. 3. A blueshift in the wavelength similar to the EL structure was observed by *ex situ* annealing of the nominally identical PL structure. Shown in red is the peak PL wavelength with annealing temperature. Shown in blue is the peak PL intensity with increasing annealing temperature; the enhancement is similar to that observed in dilute nitrides.[24–28]

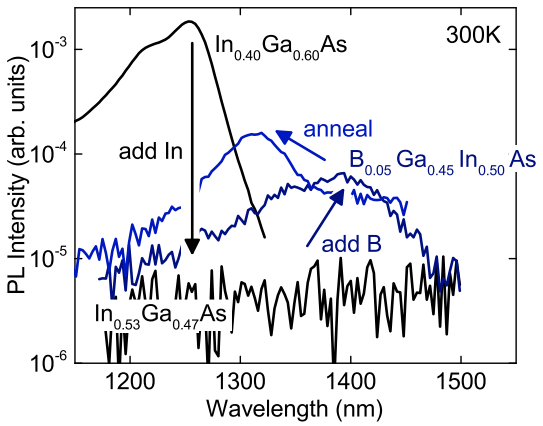

FIG. 4. PL of the (B)GaInAs QWs on GaAs targeting 1.4 μm. As expected, an InGaAs QW with the same In concentration exhibited no photoluminescence. With the addition of 5% B, wavelength extension to 1.4 μm was observed. Thermal annealing of the BGaInAs QW at 700 °C for 1 min shifted the PL peak to 1.3 μm and increased the PL intensity, demonstrating the potential for a 1.3 μm device on GaAs.

wavelength in order to account for the *in situ* annealing of the device. Increasing the as-grown emission wavelength requires the addition of indium, as well as boron to compensate the additional strain. Figure 4 shows the as-grown emission wavelength of 1.4 μm, by increasing the In concentration to 50% and the B concentration to 5%. Performing an *ex situ* annealing step at 700 °C for 1 min, we observed the peak emission wavelength blueshift to 1.3 μm and an improvement in optical quality compared to the as-grown samples. Therefore, with careful *in situ* annealing of $B_{0.05}In_{0.50}Ga_{0.45}As$ active regions, electroluminescence at 1.3 μm on GaAs is attainable.

We report a NIR, boron-containing active region electrically injected emitter. While the PL structure emitted at 1.3 μm, the EL structure emitted at <1.25 μm, likely due to the unintentional annealing of the active region during the growth of the top contact region. We confirm this with a thorough *ex situ* annealing study of our 1.3 μm PL sample, demonstrating that a true 1.3 μm emitter requires increasing the indium and boron concentration in order to account for the effects of *in situ* annealing. *Ex situ* annealing results from 1.4 μm BGaInAs emitters have blue-shifted emission at 1.3 μm after annealing, highlighting the potential of BGaInAs as the active region of 1.3 μm GaAs-based VCSELs and related devices.

This work was performed in part at the University of Texas Microelectronics Research Center, a member of the National Nanotechnology Coordinated Infrastructure (NNCI), which was supported by the National Science Foundation (No. ECCS-1542159). This work was also supported by the National Science Foundation (Award Nos. ECCS-1838984 and ECCS-1933836). Additionally, this work was supported by a Texas Instruments Fellowship and a Douglas Wilson Fellowship at the University of Texas at Austin.

DATA AVAILABILITY

The data that support the findings of this study are available from the corresponding author upon reasonable request.

REFERENCES

[1]D. L. Huffaker, G. Park, Z. Zou, O. B. Shchekin, and D. G. Deppe, Appl. Phys. Lett. **73**, 2564 (1998).
[2]K. Nakahara, M. Kondow, T. Kitatani, M. C. Larson, and K. Uomi, "1.3-μm continuous-wave lasing operation in GaInNAs quantum-well lasers," IEEE Photonics Technol. Lett. **10**, 487 (1998).
[3]A. Fiore and A. Markus, IEEE J. Quantum Electron. **43**, 287 (2007).
[4]S. G. Spruytte, M. C. Larson, W. Wampler, C. W. Coldren, H. E. Petersen, and J. S. Harris, J. Cryst. Growth **227–228**, 506 (2001).
[5]M. Kondow, K. Uomi, A. Niwa, T. Kitatani, S. Watahiki, and Y. Yazawa, Jpn. J. Appl. Phys., Part 1 **35**, 1273 (1996).
[6]G. L. Hart and A. Zunger, Phys. Rev. B **62**, 13522 (2000).
[7]M. E. Groenert, R. Averbeck, W. Hosler, M. Schuster, and H. Riechart, J. Cryst. Growth **264**, 123 (2004).
[8]J. F. Geisz, D. J. Friedman, and S. Kurtz, in Proceedings of 20th IEEE Photovoltaic Specialists Conference (2000).
[9]R. Hamila, F. Saidi, H. Maaref, P. Rodriguez, and L. Auvray, J. Appl. Phys. **112**, 063109 (2012).
[10]Q. Wang, Z. Jia, X. Ren, Y. Yan, Z. Bian, S. Cai, and Y. Huang, AIP Adv. **3**, 072111 (2013).
[11]F. Saidi, R. Hamila, H. Maaref, Ph. Rodriguez, L. Auvray, and Y. Monteil, J. Alloy Compd. **491**, 45 (2010).
[12]T. Hidouri, F. Saidi, H. Maaref, Ph. Rodriguez, and L. Auvray, Opt. Mater. **62**, 267 (2016).
[13]T. Hidouri, R. Hamila, I. Fraj, F. Saidi, H. Maaref, Ph. Rodriguez, and L. Auvray, Superlattices Microstruct. **103**, 386 (2017).
[14]A. J. Ptak, D. A. Beaton, and A. Mascarenhas, J. Cryst. Growth **351**, 122 (2012).
[15]T. Hidouri, M. Biswas, I. Mal, S. Nasr, S. Chakrabarti, D. P. Samajdar, and F. Saidi, Sol. Energy **199**, 183 (2020).
[16]T. Hidouri, S. Nasr, I. Mal, D. P. Samajdar, F. Saidi, R. Hamila, and H. Maaref, Appl. Surf. Sci. **524**, 146573 (2020).
[17]F. V. Williams and R. A. Ruehrwein, J. Amer. Chem. Soc. **82**, 1330 (1960).
[18]K. M. McNicholas, R. H. El-Jaroudi, J. Kopaczek, A. H. Jones, D. J. Ironside, R. Judrawiec, J. C. Campbell, and S. R. Bank, in Proceedings of 61st Electric Material Conference (2019).
[19]S. G. Spruytte, C. W. Coldren, A. F. Marshall, M. C. Larson, and J. S. Harris, MRS Internet J. Nitride Semicond. Res. **5**, 474 (2000).
[20]K. Volz, V. Gambin, W. Ha, M. A. Wistey, H. Yuen, S. R. Bank, and J. S. Harris, J. Cryst. Growth **251**, 360 (2003).
[21]N. Tansu, Y. L. Chang, T. Takeuchi, D. P. Bour, S. W. Corzine, M. R. T. Tan, and L. J. Mawst, IEEE Trans. Quantum Electron. **38**, 640 (2002).
[22]V. Gambin, W. Ha, M. Wistey, H. Yuen, S. R. Bank, S. M. Kim, and J. S. Harris, IEEE J. Sel. Top. Quantum Electron. **8**, 795 (2002).
[23]A. J. Ptak, S. W. Johnston, S. Kurtz, D. J. Friedman, and W. K. Metzger, J. Cryst. Growth **251**, 392 (2003).
[24]H. P. Xin, K. L. Kavanagh, M. Kondow, and C. W. Tu, J. Cryst. Growth **201-202**, 419 (1999).
[25]K. Volz, J. Koch, B. Kunert, I. Nemeth, and W. Stolz, J. Cryst. Growth **298**, 126 (2007).
[26]V. Lordi, H. B. Yuen, S. R. Bank, M. A. Wistey, S. Friedrich, and J. S. Harris, Phys. Rev. B **71**, 125309 (2005).
[27]E. V. K. Rao, A. Ougazzaden, Y. L. Bellego, and M. Juhel, Appl. Phys. Lett. **72**, 1409 (1998).
[28]T. Kageyama, T. Miyamoto, S. Makino, F. Koyama, and K. Iga, Jpn. J. Appl. Phys. Part 2 **38**, L298 (1999).